Adsorption (2014) 20:301–309
DOI 10.1007/s10450-013-9578-4

Enhanced CO_2 adsorptivity of SWCNT by polycyclic aromatic hydrocarbon intercalation

F. Khoerunnisa · D. Minami · T. Fujimori · S. Y. Hong · Y. C. Choi · H. Sakamoto · M. Endo · K. Kaneko

Received: 25 June 2013 / Accepted: 11 September 2013 / Published online: 24 September 2013
© Springer Science+Business Media New York 2013

Abstract We tuned the electronic properties of single wall carbon nanotube (SWCNT) with intercalation of naphthalene derivatives (NDs) having different electron donor or acceptor property in the SWCNT bundles. Characterization of the adsorbed SWCNT with Raman spectroscopy and electrical conductivity measurement clearly indicate the charge transfer interaction of ND molecules with SWCNT. Also X-ray diffraction supports the intercalation of ND molecules in the interstitial spaces and groove sites of SWCNT bundle. Intercalation of ND molecules enhances remarkably the CO_2 adsorptivity, which can be ascribed to the key importance of the interaction of the quadrupole moment of CO_2 with the local electrical field on the SWCNT induced by the charge transfer interaction.

Keywords CO_2 adsorptivity · Naphthalene derivatives · SWCNT · Charge transfer · Intercalation

1 Introduction

The global warming issue should be studied from a variety of scientific fields to preserve the peaceful earth. Then, predominant efforts for concentration, separation, and utilization of CO_2, being a key green house gas, have been made. As the concentration and separation of CO_2 need an efficient adsorbent for CO_2, there are active adsorption studies of CO_2 on representative nanoporous materials such as activated carbons, zeolites, and metal organic frameworks (MOFs) in addition to calcium oxides, hydrotalcites, and supported amines (Choi et al. 2009; Lastoskie 2010). Yaghi et al. showed that MOF-210 can adsorb CO_2 of 2,870 mg g^{-1} at 5.5 MPa, being much larger adsorption amount than those of zeolites and activated carbons (Millward and Yaghi 2005; Furukawa et al. 2010). Kaneko et al. found new gate adsorption of CO_2 on Cu-based MOF which can be applicable to efficient CO_2 separation (Li and Kaneko 2001; Kondo et al. 2006). On the other hand, (Silvestre-Albero et al. 2011) developed a new activated carbon which gives the excellent adsorption characteristic for CO_2 in the low pressure range below 5 MPa in comparison with the MOF-210. Still many researchers have attempted to search the better CO_2 adsorbents (Kuwahara et al. 2012; Liu et al. 2013; Llewellyn et al. 2008a, b).

CO_2 is a subcritical gas at ambient temperature, because the critical temperature is 304.25 K. Generally speaking, it is quite difficult to physically adsorb the supercritical gas or subcritical gas sufficiently even on nanoporous materials, since physical adsorption is a predominant process only for vapors even on the nanoporous materials. Introduction of a weak chemisorption-type interaction between the supercritical gas and nanoporous material is indispensable. Therefore, we must elucidate key factors for enhancement of physical adsorption of CO_2 with nanoporous materials. One of authors succeeded to develop an excellent carbon adsorbent for supercritical NO through promotion of the NO dimerization with the aid of the pore-entrance modification with nanoscale iron oxides (Kaneko 1987a; Kaneko et al. 1987b). In this case, the interaction of an

F. Khoerunnisa · D. Minami · T. Fujimori · H. Sakamoto · M. Endo · K. Kaneko (✉)
Research Center for Exotic Nanocarbons, Shinshu University, 4-17-1 Wakasato, Nagano 380-8553, Japan
e-mail: kkaneko@shinshu-u.ac.jp

F. Khoerunnisa
Department of Chemistry, Indonesia University of Education, Bandung 40154, Indonesia

S. Y. Hong · Y. C. Choi
Research and Development Center, Hanwha Nanotech, Bupyeong-gu, Inchon 403-030, Republic of Korea

electron spin of the NO molecule with the local magnetic field of the iron oxide enhances the NO dimerization. CO_2 has a large quadrupole moment, although the CO_2 molecule has no unpaired electron. The quadrupole moment of CO_2 is -14.9×10^{-40} C m^2, whereas those of N_2 and O_2 are -4.90×10^{-40} and -1.33×10^{-40} C m^2, respectively (Rigby et al. 1986). Consequently, we can expect that a local electric field on the nanopore wall is efficient for enhancement of CO_2 adsorption.

It is well-known that polyaromatic hydrocarbons (PAHs) interact strongly with single wall carbon nanotube (SWCNT) (Hattori et al. 2013; Debnath et al. 2010; Sundramoorthy et al. 2013; Zilberman et al. 2011). Gotovac et al. studied systematically adsorption of PAHs on SWCNT, showing the presence of charge transfer interaction between PAH and SWCNT (Gotovac et al. 2006, 2007). In particular, they found that intercalation of naphthalene molecules in the SWCNT bundle brought about metallicity with the aid of ultraviolet photoelectron spectroscopy, indicating a marked charge transfer interaction (Gotovac-Atlagić et al. 2010). Consequently, we can tune the induced charge of the SWCNT walls with doping of naphthalene derivatives (NDs) having different electron donor and acceptor properties. Additionally, Zhang et al. reported that the electronic interaction of anthracene derivatives adsorbed with sidewalls of SWCNT was evidenced by the red shifts of photoemission peak of absorptive adducts, being consistent with charge-transfer interaction (Zhang et al. 2003). This topic also promoted the modification study on electronic properties of SWCNT with PAHs adsorption (Shin et al. 2008; Hasobe 2012; Tasis et al. 2009).

Moreover, we showed that the surface charge-donation with encapsulated dye molecules increased CO_2 adsorptivity of SWCNT (Khoerunnisa et al. 2012). Hence, we must clarify the essential factors influencing CO_2 adsorption on carbon nanotubes through exploring other PAH molecules that can modulate the electronic structure of nanotube by changing the π-electron density. In the present study, we selected following NDs of different electron donor and acceptor characteristics for coating SWCNT (Shin et al. 2008). The different functional moieties of naphthalene such as hydroxyl (–OH), amine (–NH_2), methyl (–CH_3) and nitro (–NO_2) were used to investigate the contribution of surface charge donation on enhancement of CO_2 adsorptivity of SWCNT.

2 Experimental

2.1 Materials

SWCNT prepared by Hanwha Nanotech Co. The SWCNT was purified with 1 M HCl for 20 h at room temperature and dried at 373 K after washing. SWCNT sample was annealed at 1,473 K under Ar for 30 min for removal of amorphous carbon. The tube diameter of the purified-SWCNT determined by Raman RBM analysis (laser excitation of 532 nm) is in the range of 1.33–1.60 nm. ND with the purity over 99.8 and 98 %, respectively, were purchased from Tokyo Chemical Industry (TCI) Co. Ltd and used without further purification. These The NDs of 1,5-dihydroxynaphthalene ($C_{10}H_8O_2$), 1,5-diaminonaphthalene ($C_{10}H_{10}N_2$), 1,5-dimethylnaphthalene ($C_{12}H_{12}$), 1,5-dinitronaphthalene ($C_{10}H_6N_2O_4$) are denoted as DHN, DAN DMN, and DNN, respectively, in this articles.

2.2 NDs-intercalated SWCNT

Intercalation of ND in SWCNT was carried out with liquid phase adsorption at 298 K. ND solutions were prepared by dissolving ND compounds into 50 mL of toluene. The SWCNT of 5 mg was ultrasonically dispersed in 50 mL of ND solution at 298 K for 48 h. The dispersed SWCNT samples after adsorption were filtrated with a Millipore porous filter (0.45 μm) and washed by 100 mL of toluene at 298 K under vacuum for 1 h to remove any non-adsorbed naphthalene and ND molecules. The ND-adsorbed SWCNT samples were dried before characterization under vacuum (1 Pa) for 24 h. The ND adsorption amount was determined from the concentration change of ND molecules in the solution using the UV–Vis-NIR spectrometer (JASCO; V-670). The surface coverage of SWCNT with ND molecules was evaluated from adsorbed molecules of ND divided by the surface area of SWCNT.

2.3 Characterization

The X-ray diffraction patterns of ND-adsorbed SWCNTs were measured at room temperature using the X-ray diffractometer (RINT-2300SF, Rigaku) with MoKα at 50 kV and 300 mA. The SEM images were taken by means of field emission scanning electron microscope (FE-SEM; JSM-6330F, JEOL). The nanoporosity and adsorption activity change of SWCNT with ND adsorption were examined with N_2 adsorption at 77 K (Autosorb iQ; Quantachrome) and CO_2 adsorption at 293 K (Belsorp-max, Bel Japan Inc.), respectively, after preheating at 423 K and 10^{-4} Pa for 2 h. Infrared spectra were measured over the range of 1,000–4,000 cm^{-1} by placing the sample on KBr plate with the aid of an FTIR spectrometer (Nicolet 6700, Thermo Scientific) under atmospheric conditions. Each spectrum was 40 scans collected at a resolution of 2 cm^{-1}. The Raman spectra were measured under ambient conditions using a Raman spectrometer (InVia Raman microscope, Renishaw) equipped with diode laser (power 0.3 mW, wavelength 785 nm). The compression pressure

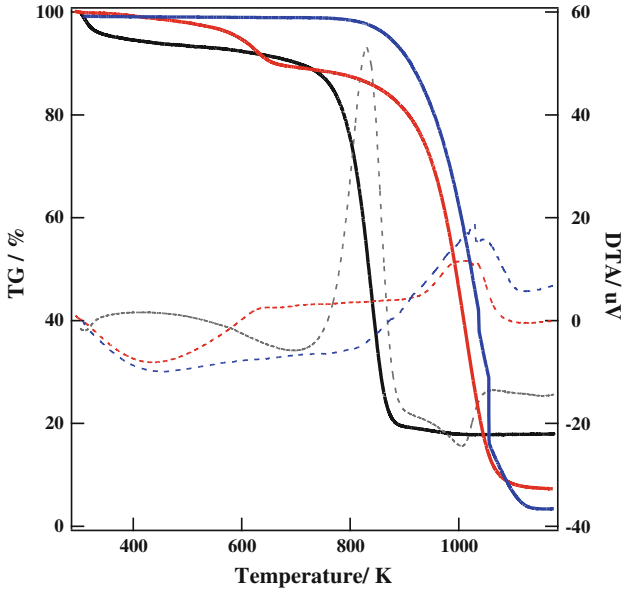

Fig. 1 TG and differential thermal analysis (DTA) curves of SWCNT samples indicated by *solid* and *dash lines*, respectively: As-received (*black*), acid treated (*red*), and acid annealing treated (*blue*) SWCNT samples (Color figure online)

dependence of dc electrical conductivity of ND-adsorbed SWCNT was measured at 298 K with the aid of four probes apparatus in vacuum. The impurity amount of SWCNT was evaluated by the thermal gravimetry (TG) over the temperature range of 303–1,200 K in a flow of O_2–N_2 mixed gas at 300 mL min^{-1} with the heating rate of 3 K min^{-1} (Thermo Plus, TG 8120, Rigaku).

3 Results and discussion

3.1 Charge transfer interaction between ND molecules and SWCNT

The thermal gravimetric profile shows the efficient removal of impurities and amorphous carbon of SWCNT with the acid and high temperature-annealing treatments, as shown on Fig. 1. The SWCNT samples are highly purified through two-step treatment of acid and highly temperature annealing treatments. The metallic impurity is 3 wt%. The surface coverage (θ) of the ND adsorbed SWCNT samples was controlled to be the constant value of 0.30 ± 0.01 for all samples.

Figure 2 shows SEM images of SWCNT and ND-adsorbed SWCNT. The SEM images of SWCNT exhibits highly bundled structures that are randomly entangled with each other. The ND adsorption-treatment induces a partial unraveling of the bundle structure, suggesting the specific interaction between ND molecules and SWCNT. Figure 3 show the X-ray diffraction pattern of SWCNT, which has a well-ordered two-dimensional hexagonal lattice of the bundle structure. The predominant peak at 2.72° is assigned to the 10 peak of the hexagonal lattice. The other diffraction peaks at 4.40°, 7.06°, and 9.56° correspond to the reflections from the 11, 20, and 21 lattice planes, respectively; the peak at around 11.90° is attributed to the well-defined reflection from the graphite 002 lattice planes, being as an impurity. As almost all SWCNT samples have cap structures even after the purification treatment according to the N_2 adsorption at 77 K described later, ND molecules can be mainly adsorbed on the external surface of the bundles, the groove sites and the interstitial pore spaces of the bundle. Also ND molecules can interact strongly with the conjugated π-electron surface and thereby ND molecules should be intercalated in the interstitial spaces. This is suggested from the fact that the intercalation unravels the bundle structure as shown by SEM observation. The intercalation of ND molecules in the interstitial spaces and/or the groove sites of SWCNT was evidenced by a lower angle shift, depression and broadening of the 10 peak of the X-ray diffraction, indicating the expansion of the interstitial spaces and partial disordering of the bundles of the hexagonal symmetry. The 10 peak shift corresponds to the increase of the interlayer spacing of the 10 planes by 0.063–0.113 nm. Then, the half of interlayer spacing of the 10 planes is in the range of 0.78–0.81 nm which is larger than the short molecular axis-width of the ND molecules (0.55–0.67 nm). Consequently the ND molecule can be accepted in the expanded 10 layer-spaces, as illustrated in Fig. 4. Figure 4 shows a model local arrangement of SWCNT bundle of which hexagonal symmetry is partially broken to embrace the ND molecule. The scattering parameters of ND-adsorbed SWCNT are summarized in Table 1.

The FTIR spectrum of SWCNT in Fig. 5 shows the typical vibration modes of carbon nanotubes around 3,450, 2,920 and 2,850, and 1,640 cm^{-1} being assigned to the stretching vibration modes of O–H, C–H of methylene group, and C=C of benzene ring, respectively. The ND adsorption on SWCNT induces the remarkable frequency shifts, especially for O–H and C=C vibration. In addition, the new peaks appear at 1,385 and 1,468 cm^{-1} due to the stretching vibration modes of C–H from phenyl group. These results suggest the strong interaction of ND molecules with SWCNT walls. Furthermore, the change in the radial breathing mode (RBM) of Raman spectra on the ND-adsorption as shown in Fig. 6 indicates interaction between SWCNT and ND molecules. In particular, the donating moieties such as $–CH_3$, $–NH_2$, and –OH induce a notably higher frequency shift of RBM, while DNN of an acceptor one does not show any shift in RBM peak. The shifts should stem from the charge transfer interaction between ND

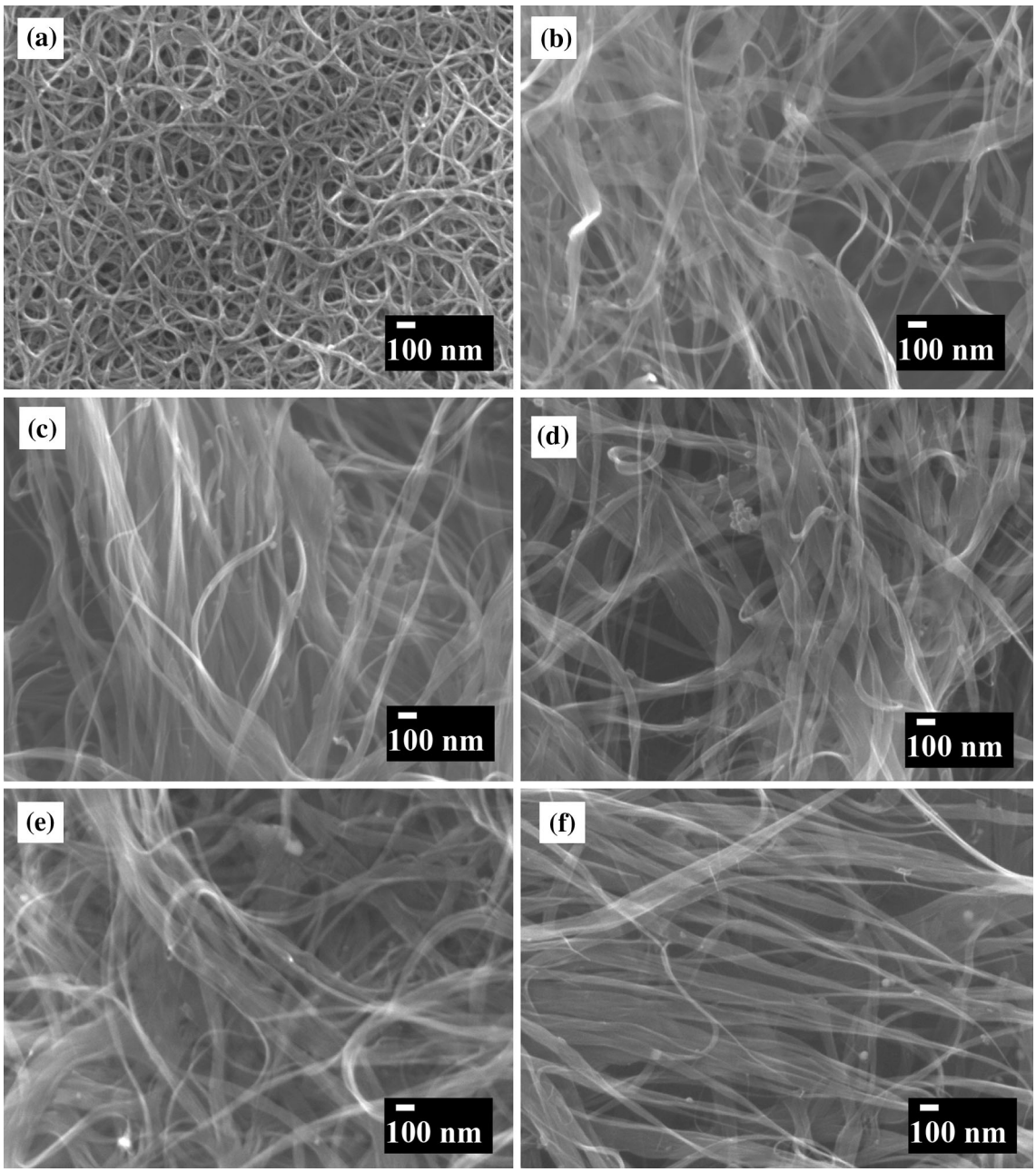

Fig. 2 SEM images of SWCNT and ND-adsorbed SWCNT: SWCNT (**a**), DHN-SWCNT (**b**), DAN-SWCNT (**c**), DMN-SWCNT (**d**), N-SWCNT (**e**), and DNN-SWCNT (**f**)

molecules and SWCNT-wall, leading to the perturbation of radial flexibility of aromatic rings in the tube structure known as the mode hardening effect (Gotovac et al. 2007). Figure 7 shows Raman G-bands of SWCNT and ND-adsorbed SWCNT. All G-bands have G^- and G^+ components around 1,570 and 1,590 cm^{-1}, respectively. Here the G^- feature is sensitive to metallic or semiconducting state of SWCNT. If SWCNT is metallic, the G^- band should be very broad. In this case, all samples are mixture of metallic and semiconducting SWCNTs and thereby the difference in the G^- feature due to the ND-adsorption is not explicit.

Moreover, Fig. 8 shows the compression pressure dependence of dc electrical conductivity of ND-adsorbed SWCNT at room temperature. The ND-adsorption markedly increases electrical conductivity of SWCNT, indicating an evident charge transfer interaction between ND molecules and SWCNT.

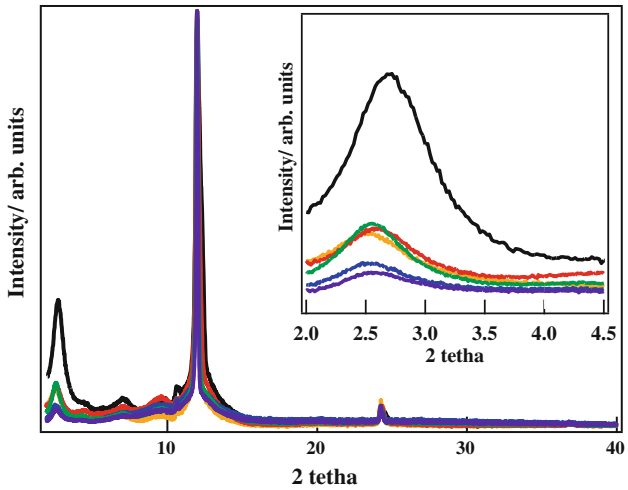

Fig. 3 The X-ray diffraction patterns of SWCNT and ND-adsorbed SWCNT: SWCNT (*black*), DHN-SWCNT (*red*), DAN-SWCNT (*blue*), DMN-SWCNT (*green*), N-SWCNT (*purple*), and DNN-SWCNT (*yellow*). *Inset* magnified XRD patterns in the low scattering angle region (Color figure online)

3.2 Nanoporosity of NDs-intercalated SWCNT

The porosity change of SWCNT on ND adsorption was evaluated by nitrogen adsorption at 77 K. The adsorption isotherms of nitrogen on SWCNT samples are of IUPAC type II, as shown in Fig. 9. The initial adsorption uptake stems from micropore filling of N_2 mainly in the interstitial tube spaces. We observed a marked adsorption hysteresis which can be ascribed to limited diffusion of N_2 molecules in the interstitial tube spaces. The adsorption of nitrogen in a higher P/Po region derives from multilayer adsorption on the pore walls of larger mesopores and macropores due to interbundle gaps and on the external surface of the bundles. The intercalation of ND molecules decreases the initial adsorption uptake markedly and the adsorption isotherm of ND-adsorbed SWCNT just shifts downward, indicating that ND molecules are preferentially adsorbed in the interstitial spaces accompanying with the slight expansion of the interstitial spaces, because those are the strongest

Table 1 The interlayer spacing (d) and crystallite sizes (L) of SWCNT and ND-adsorbed SWCNT

Sample	2θ	d (nm)	L (nm)
SWCNT	2.72	1.497	8
DHN-SWCNT	2.61	1.560	6
DAN-SWCNT	2.55	1.597	5
DMN-SWCNT	2.55	1.597	7
N-SWCNT	2.55	1.597	5
DNN-SWCNT	2.53	1.610	6

adsorption sites in the SWCNT bundles. The nitrogen adsorption data also support the interaction of ND molecules in the SWCNT bundle. The pore structure parameters were evaluated with the subtracting pore effect (SPE) method using high resolution α_s plots of nitrogen adsorption at 77 K (Kaneko et al. 1992a; Kaneko and Ishii 1992b). The pore structure parameters of SWCNT and ND-intercalated SWCNT are summarized in the Table 2. The ND-adsorption treatment decreases markedly the surface area and micropore volume. This support the interaction in the interstitial pore spaces, because the ND molecules block the interstitial pores.

3.3 CO_2 adsorptivity change of SWCNT with ND-intercalation

The CO_2 adsorption is an effective technique to evaluate narrow micropores. In particular, characterization with CO_2 adsorption is fit for microporous carbons which give the N_2 adsorption isotherm of the low pressure marked adsorption hysteresis as observed in Fig. 9a. Also CO_2 has a large quadrupole moment compared with N_2 and O_2, as described in Introduction. CO_2 adsorptivity should be sensitive to surface charged state due to the interaction of the quadrupole moment of CO_2 with the local surface electric field. It is well-known that metal oxide surfaces having surface charges gives a great difference in isosteric heat of adsorption for N_2 and Ar by 3–5 kJ mol^{-1}, which

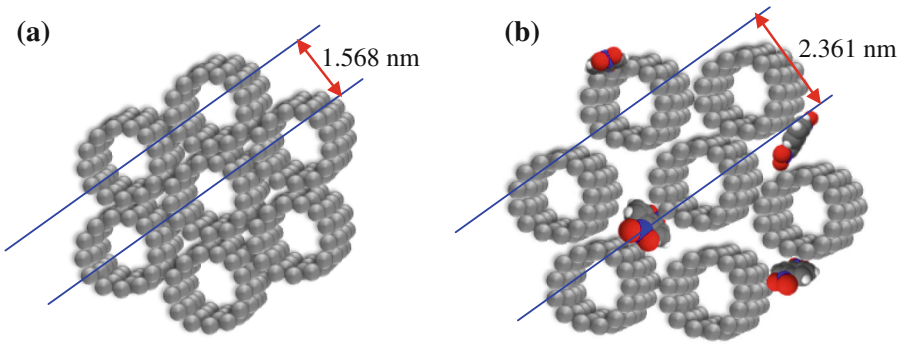

Fig. 4 Model of local destruction of the symmetrical bundle structure on intercalation of a ND molecule: **a** SWCNT bundle and **b** ND-adsorbed SWCNT

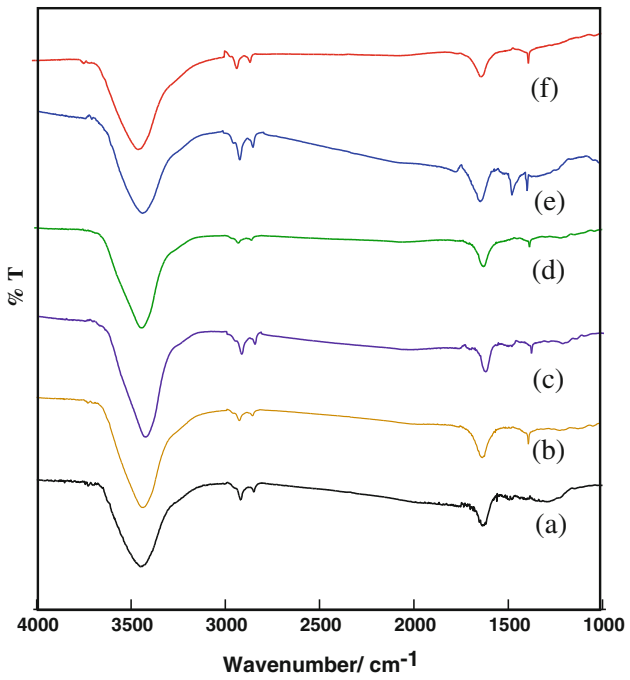

Fig. 5 FTIR spectra of SWCNT and ND-adsorbed SWCNT: SWCNT (*a*), DNN-SWCNT (*b*), N-SWCNT (*c*), DMN-SWCNT (*d*), DAN-SWCNT (*e*), and DHN-SWCNT (*f*)

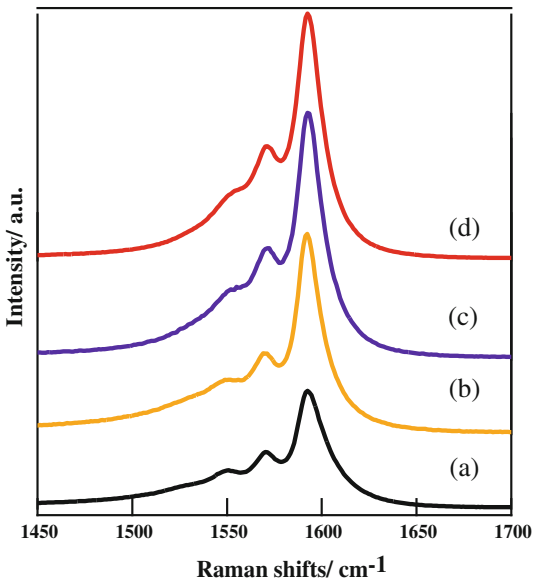

Fig. 7 Raman G-bands with laser 785 nm of SWCNT and ND-adsorbed SWCNT: SWCNT (*a*), DNN-SWCNT (*b*), N-SWCNT (*c*), and DHN-SWCNT (*d*)

corresponds to more than 40 % of the isosteric heat of Ar adsorption (Gregg and Sing 1982). As Ar has no quadrupole moment, even the smaller quadrupole moment of the N_2 molecule than CO_2 leads to such a large contribution to adsorption. Consequently we can expect an explicit influence of the surface charge on CO_2 adsorption for ND-adsorbed SWCNT. In this work, we prepared the intercalated SWCNT with ND having different electron donor and acceptor properties; DHN, DAN, and DMN should donate negative charge on SWCNT, while SWCNT should have positive charges on DNN adsorption treatment. The electrical conductivity results indicate that the DNN-intercalation is the most effective for charge transfer interaction with SWCNT. Then, the pore walls of DNN-SWCNT should have highly and positively charged. Therefore, we expect the most remarkable enhancement of CO_2 adsorption. Briefly speaking, the intercalation of naphthalene and NDs gives rise to predominant enhancement of CO_2 adsorption, as shown in Fig. 10. Here CO_2 adsorbed amount of Fig. 10 is normalized by the pore volume obtained from N_2 adsorption. Particularly, intercalation

Fig. 6 Raman RBM with laser 785 nm of SWCNT and ND-adsorbed SWCNT: SWCNT (*a*), DNN-SWCNT (*b*), N-SWCNT (*c*), DMN-SWCNT (*d*), DAN-SWCNT (*e*), and DHN-SWCNT (*f*)

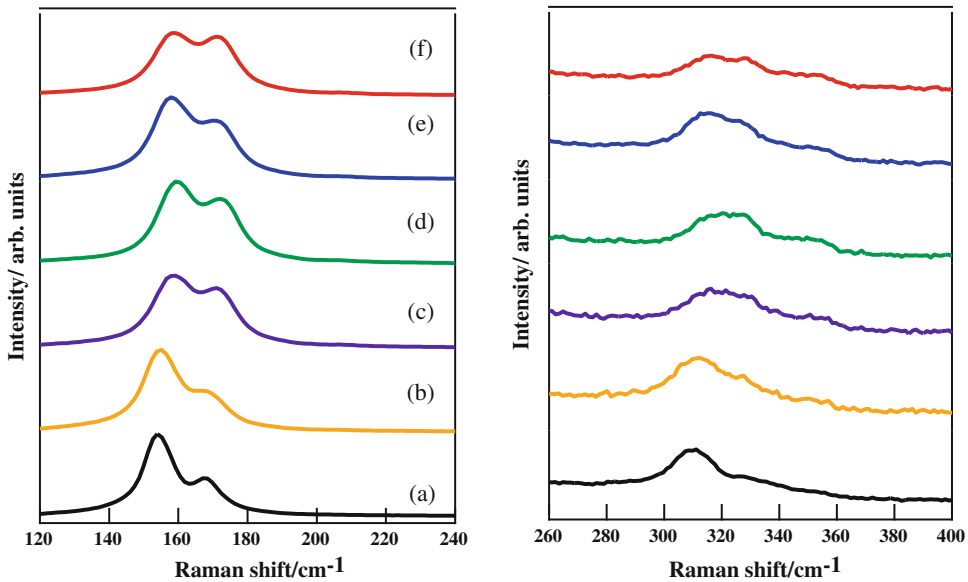

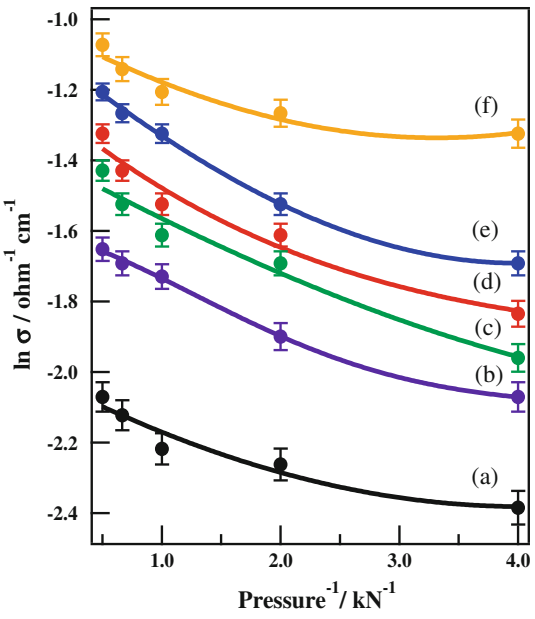

Fig. 8 Pressure dependence of electrical conductivity of SWCNT and ND-adsorbed SWCNT at room temperature: SWCNT (*a*), N-SWCNT (*b*), DMN-SWCNT (*c*), DHN-SWCNT (*d*), DAN-SWCNT (*e*), and DNN-SWCNT (*f*)

with ND of electron donor moieties such as hydroxyl and amine significantly enhances CO_2 adsorptivity, being different from the above expectation.

We must take into account the dispersion interaction, orientation of the CO_2 molecules, and localized charges on the surface moiety for better understanding the observed results. The major attractive interaction of the CO_2 molecules and SWCNT comes from dispersion interaction and then the parallel orientation (in-plane) of the CO_2 molecules to the pore wall is more favored than the perpendicular orientation (out-of-plane) against the pore wall in the dispersion interaction. Then adsorbed CO_2 molecules must be lying on the pore walls. The interaction of the quadrupole moment of CO_2 with the local surface electric field can contribute to more stabilize CO_2 on SWCNT in addition to the dispersion interaction. The interaction of the CO_2 quadrupole moment with the surface electric field is influenced by the molecular orientation against the pore wall as well as the dispersion interaction; the in-plane CO_2 molecule is also preferable in this interaction. This is because the doubly charged positive pole and mono charged negative poles of the quadruple of CO_2 are situated

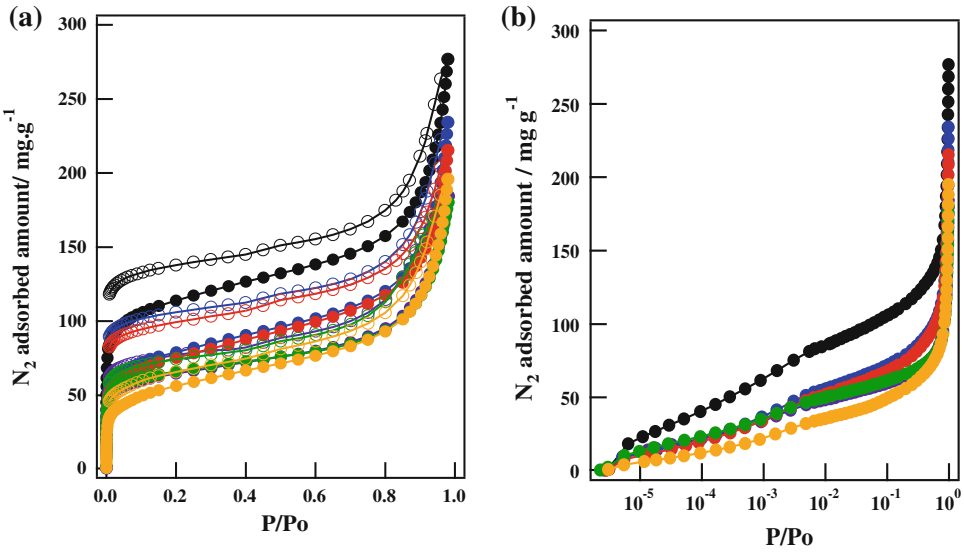

Fig. 9 The N_2 adsorption isotherms at 77 K of SWCNT and ND-adsorbed SWCNT: **a** linear plot and **b** logarithmic plot. SWCNT (*black*), DHN-SWCNT (*red*), DAN-SWCNT (*blue*), DMN-SWCNT (*green*), N-SWCNT (*purple*), and DNN-SWCNT (*yellow*). Adsorption and desorption branches are indicated by the *filled* and *open circles*, respectively in (**a**). The desorption branches are not shown for clarity in (**b**) (Color figure online)

Table 2 Pore structure parameters determined by SPE method

Sample	S_t (m^2 g^{-1})	V_t (mL g^{-1})	S_{pore} (m^2 g^{-1})	S_{ext} (m^2 g^{-1})	V_{micro} (mL g^{-1})	V_{meso} (mL g^{-1})
SWCNT	330	0.34	250	80	0.14	0.19
DHN-SWCNT	230	0.31	140	90	0.11	0.18
DAN-SWCNT	200	0.29	120	80	0.10	0.17
DMN-SWCNT	190	0.22	140	50	0.08	0.15
N-SWCNT	180	0.23	130	50	0.08	0.15
DNN-SWCNT	150	0.24	80	70	0.06	0.18

Here S_t, S_{pore}, and S_{ext} are the total surface area, pore surface area, and external surface area, respectively. V_t, V_{micro}, and V_{meso} are the total pore volume, micropore volume, and mesopore volume, respectively

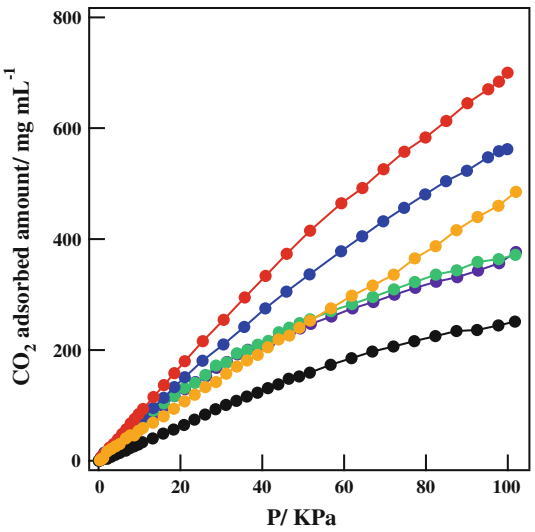

Fig. 10 CO_2 adsorption isotherms at 293 K of SWCNT and ND-adsorbed SWCNT: SWCNT (*black*), DHN-SWCNT (*red*), DAN-SWCNT (*blue*), DMN-SWCNT (*green*), N-SWCNT (*purple*), and DNN-SWCNT (*yellow*) (Color figure online)

at the carbon atom and oxygen atoms, respectively. Possibly the positive poles of the in-plane CO_2 can have greater attractive interaction energy than the negative pole of the out-of-plane CO_2. Accordingly, the negatively charged walls of electron donor-intercalated SWCNT can have larger stabilization energy than the positively charged wall of DNN-SWCNT. Also the in-plane CO_2 is allowed by geometrical restriction of the interstitial pores and the groove sites of the SWCNT bundles.

We need discuss on the effect of localized charges on the surface moiety, which should bring about additional CO_2 adsorption. In this case, DHN of hydroxyl groups is more effective than DAN of amino groups, although surface modification with amine groups is generally the most efficient for improvement of CO_2 adsorptivity (Su et al. 2011; Plaza et al. 2007; Serna-Guerrero et al. 2008; Zhang et al. 2010; Wang and Yang 2012). Surface amines can interact strongly with CO_2 through the formation of carbamate under the dry conditions (Serna-Guerrero et al. 2008) and thereby the amine-mediated strong adsorption of CO_2 needs enough room for formation of the carbamte. Even reversible hydrogen bonding associated interaction of amine with CO_2 should be perturbed by the pore space restriction (Hicks et al. (2008). On the other hand, the electrostatic interaction stemming from the quadrupole moment of CO_2 and the local electric field at hydroxyl group can choose flexible configuration between CO_2 and the hydroxyl of the DHN. This is one of plausible reasons why DHN-SWCNT has the higher CO_2 adsorptivity than DMN-SWCNT. As DMN has no local charge on CH_3 moiety, the enhancement of CO_2 adsorption of DMN-SWCNT is not so marked compared with DHN-SWCNT and DAN-SWCNT. Thus, we can understand the CO_2 adsorption enhancement by the ND interaction, although comparison of CO_2 adsorptivity of DNN-SWCNT with that of DMN-SWCNT is still difficult. In future, we must introduce molecular simulation to get information on the most plausible intercalation structure and micropore structural change due to the interaction of NDs.

4 Conclusion

We have shown the distinctive interfacial properties of SWCNT tuned with NDs intercalation. The ND molecules were intercalated in the expanded interstitial spaces of SWCNT bundles which are proven by X-ray diffraction and N_2 adsorption porosimetry. Raman scattering and electrical conductivity measurements revealed the charge transfer interaction between NDs and SWCNT. Intercalation treatment with ND molecules suggests a new guideline for designing better CO_2 adsorbents. The remarkably increased CO_2 adsorptivity of SWCNT by the ND intercalation was due to the additional electrostatic interaction between the quadrupole moment of CO_2 molecules and the pore wall. The hydroxyl moieties showed the most significant effect in the enhancement of CO_2 adsorptivity, although we do not understand exactly the contribution of the microporosity difference in the ND-intercalated SWCNT samples yet.

Acknowledgments K. K., T. F., D. M, and H. S., were supported by Exotic Nanocarbons, Japan Regional Innovation Strategy Program by the Excellent, JST. This work was supported by the Grant-in-Aid for Scientific Research (A) (No. 24241038) by JSPS.

References

Choi, S., Drese, J.H., Jones, C.W.: Adsorbent materials for carbon dioxide capture from large anthropogenic point sources. ChemSusChem **2**, 796–854 (2009). doi:10.1002/cssc.200900036

Debnath, S., Cheng, Q., Hedderman, T.G., Byrne, H.J.: Comparative study of the interaction of different polycyclic aromatic hydrocarbons on different types of single-walled carbon nanotubes. J. Phys. Chem. C **114**, 8167–8175 (2010)

Furukawa, H., Ko, N., Go, Y.B., Aratani, N., Choi, A.B., Choi, E., Yazaydin, A.O., Snurr, R.Q., Keefee, M.O., Kim, J., Yaghi, O.M.: Ultrahigh porosity in metal-organic frameworks. Science **329**, 424–428 (2010)

Gregg, S.J., Sing, K.S.W.: Adsorption, surface area and porosity, p. 12. Academic Press, London (1982)

Gotovac, S., Hattori, Y., Noguchi, D., Miyamoto, J., Kanamaru, M., Utsumi, S., Kanoh, H., Kaneko, K.: Phenanthrene adsorption from solution on single wall carbon nanotube. J. Phys. Chem. B **110**, 16219–16224 (2006)

Gotovac, S., Honda, H., Hattori, Y., Takahashi, K., Kanoh, H., Kaneko, K.: Effect of nanoscale curvature of single-walled carbon nanotubes on adsorption of polycyclic aromatic hydrocarbons. Nano Lett. **7**(3), 583–587 (2007)

Gotovac-Atlagić, S., Hosokai, T., Ohba, T., Ochiai, Y., Kanoh, H., Ueno, N., Kaneko, K.: Pseudometallization of single wall carbon

nanotube bundles with intercalation of naphthalene. Phys. Rev. B **82**, 075136-1-6 (2010)

Hattori, Y., Kaneko, K., Ohba, T.: Comprehensive inorganic chemistry II, vol. 5, pp. 25–44. Elsevier, Oxford (2013)

Hasobe, T.: Photo- and electron-functional self-assembled architectures of porphyrins. Phys. Chem. Chem. Phys. **14**, 15975–15987 (2012)

Hicks, J.C., Drese, J.H., Fauth, J.F., Gray, M.L., Qi, G., Jones, C.W.: Desinging adsorbents for CO_2 capture from flue gas-hyperbranched aminosilicas capable of capturing CO_2 reversibly. J. Am. Chem. Soc. **130**, 2902–2903 (2008)

Kaneko, K.: Anomalous micropore filling of NO on α-FeOOH-dispersed activated carbon fibers. Langmuir **3**, 357–363 (1987a)

Kaneko, K., Fukuzaki, N., Ozeki, S.: The concentrated NO dimer in micropores above room temperature. J. Chem. Phys. **87**, 776–777 (1987b)

Kaneko, K., Ishii, C., Ruike, M., Kuwabara, H.: Origin of superhigh surface area and microcrystalline graphitic structures of activated carbons. Carbon **30**, 1075–1088 (1992a)

Kaneko, K., Ishii, C.: Superhigh surface area determination of microporous solids. Colloid Surf. **67**, 203–212 (1992b)

Khoerunnisa, F., Fujimori, T., Itoh, T., Urita, K., Hayashi, T., Kanoh, H., Ohba, T., Hong, S.Y., Choi, Y.C., Santosa, S.J., Endo, M., Kaneko, K.: Enhanced CO_2 adsorptivity of partially charged single walled carbon nanotubes by methylene blue encapsulation. J. Phys. Chem. C **116**, 11216–11222 (2012)

Kondo, A., Noguchi, H., Ohnishi, S., Kajiro, H., Tohdoh, A., Hattori, Y., Xu, W.-C., Tanaka, H., Kanoh, H., Kaneko, K.: Novel expansion/shrinkage modulation of 2D layered MOF triggered by clathrate formation with CO_2 molecules. Nano Lett. **6**(11), 2581–2584 (2006)

Kuwahara, Y., Kang, D.-Y., Copeland, J.R., Brunelli, N.A., Didas, S.A., Bollini, P., Sievers, C., Kamegawa, T., Yamashita, H., Jones, C.W.: Dramatic enhancement of CO_2 uptake by poly(ethyleneimine) using zirconosilicate support. J. Am. Chem. Soc. **134**, 10757–10760 (2012)

Lastoskie, C.: Caging carbon dioxide. Science **330**, 595–596 (2010)

Li, D., Kaneko, K.: Hydrogen bond-regulated microporous nature of copper complex-assembled microcrystals. Chem. Phys. Lett. **335**, 50–56 (2001)

Liu, Y.-Y., Couck, S., Vandichel, M., Grzywa, M., Leus, K., Biswas, S., Volkmer, D., Gascon, J., Kapteijn, F., Denayer, J.F.M., Waroquier, M., Speybroeck, V.V., Voort, P.V.D.: New VIV-based metal-organic framework having framework flexibility and high CO_2 adsorption capacity. Inorg. Chem. **52**, 113–120 (2013)

Llewellyn, P.L., Bourrelly, S., Serre, C., Vimont, A., Daturi, M., Hamon, L., Weireld, G.D., Chang, J.-S., Hong, D.-Y., Hwang, Y.K., Jung, S.H., Ferey, G.: High uptakes of CO_2 and CH_4 in mesopores metal organic frameworks MIL-100 and MIL-101. Langmuir **24**, 7245–7250 (2008a)

Llewellyn, P.L., Maurin, G., Devic, T., Serna, S.L., Rosenbach, N., Serre, C., Bourrellly, S., Horcajada, P., Filinchuk, Y., Fereys, G.: Prediction of the condition for breathing of metal organic framework materials using combination of X-ray powder diffraction, microcalorimetry, and molecular simulation. J. Am. Chem. Soc. **130**, 12808–12814 (2008b)

Millward, A.R., Yaghi, O.M.: Metal-organic frameworks with exceptionally high capacity for storage of carbon dioxide at room temperature. J. Am. Chem. Soc. **127**, 17998–17999 (2005)

Plaza, M.G., Pevida, C., Arenillas, A., Rubiera, F., Pis, J.J.: CO_2 capture by adsorption with nitrogen enriched carbons. Fuel **86**, 2204–2212 (2007)

Rigby, M., Smith, E.B., Wakeham, W.A., Maitland, G.C.: The Forces between molecules, p. 188. Oxford, New York (1986)

Serna-Guerrero, R., Da'na, E., Dayari, A.: New insights into interactions of CO_2 with amine-functionalized silica. Ind. Eng. Chem. Res. **47**, 9406–9412 (2008)

Shin, H.-J., Kim, S.M., Yoon, S.-M., Benayad, A., Kim, K.K., Kim, S.J., Park, H.K., Choi, J.-Y., Lee, Y.H.: Tailoring electronic structures of carbon nanotubes by solvent with electron-donating and withdrawing groups. J. Am. Chem. Soc. **130**, 2062–2066 (2008)

Silvestre-Albero, J., Wahby, A., Sepúlveda-Escribano, A., Martínez-Escandell, M., Kaneko, K., Rodríguez-Reinoso, F.: Ultrahigh CO_2 adsorption capacity on carbon molecular sieves at room temperature. Chem. Comm. **47**, 6840–6842 (2011)

Su, F., Lu, C., Chen, H.-S.: Adsorption, desorption and thermodynamic studies of CO_2 with high-amine-loaded multiwalled carbon nanotubes. Langmuir **27**(13), 8090–8098 (2011)

Sundramoorthy, A.K., Mesgari, S., Wang, J., Kumar, R., Sk, M.A., Yeap, S.H., Zhang, Q., Sze, S.K., Lim, K.H., Park, M.B.C.: Scalable and effective enrichment of semiconducting single-walled carbon nanotubes by a dual selective naphthalene-based azo dispersant. J. Am. Chem. Soc. **135**, 5569–5581 (2013). doi:10.1021/ja312282g

Tasis, D., Mikroyannidis, J., Karoutsos, V., Galiotis, C., Papagelis, K.: Single-walled carbon nanotubes decorated with a pyrene–fluorenevinylene conjugate. Nanotechnology **20**, 135606 (2009)

Wang, L., Yang, R.T.: Significantly increased CO_2 adsorption performance of nanostructured templated carbon by tuning surface area and nitrogen doping. J. Phys. Chem. C **116**, 1099–1106 (2012)

Zhang, J., Lee, J.-K., Wu, Y., Murray, R.W.: Photoluminescence and electronic interaction of anthracene derivatives adsorbed on sidewalls of single-walled carbon nanotubes. Nano Lett. **3**(3), 403–407 (2003)

Zhang, Z., Xu, M., Wang, H., Li, Z.: Enhancement of CO_2 adsorption on high surface area activated carbon modified by N_2, H_2, and ammonia. Chem. Eng. J. **160**, 57–577 (2010)

Zilberman, Y., Ionescu, R., Feng, X., Müllen, K., Haick, H.: Nanoarray of polycyclic aromatic hydrocarbons and carbon nanotubes for accurate and predictive detection in real-world environmental humidity. ACS Nano **5**(8), 6743–6753 (2011)